

Statistical n-butyl acrylate–sulphonatopropylbetaine copolymers: 1. Synthesis and molecular characterization

Marc Ehrmann and Jean-Claude Galin*

Institut Charles Sadron, CRM-EAHP, CNRS-ULP, 6 rue Boussingault,
67083 Strasbourg Cedex, France

(Received 11 December 1990; accepted 13 February 1991)

Radical copolymerization of n-butyl acrylate (A) and 1,1-dimethyl-1-(3-methacrylamidopropyl)-1-(3-sulphopropyl)ammonium betaine (B) initiated by 4,4'-azobis-4-cyanovaleric acid (ACVA) was studied in ethanol solution at 50°C: $[A + B] \approx 1-2.9 \text{ mol l}^{-1}$ (molar fraction of monomer B, $f_B \leq 0.65$), $[ACVA] = 1 \times 10^{-3} \text{ mol l}^{-1}$. The copolymerization process apparently obeys the terminal unit model over the whole composition range ($r_A = 0.42$, $r_B = 6.0$), and the reliability of these reactivity ratios was checked through the analysis of the monomer unit distribution in the chain by ^{13}C nuclear magnetic resonance spectroscopy (carbonyl pattern). For constant concentrations in monomers and initiator, the transition from a homogeneous to a heterogeneous system for $f_B = 0.1$ leads to a twofold increase in the average degree of polymerization with respect to pure poly(n-butyl acrylate). The B units slightly increase the sensitivity of the copolymer to thermal degradation (initial degradation temperature of 300°C under nitrogen).

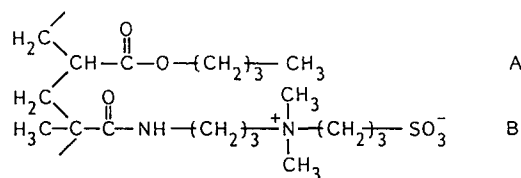
(Keywords: radical copolymerization; n-butyl acrylate; 1,1-dimethyl-1-(3-methacrylamidopropyl)-1-(3-sulphopropyl)ammonium betaine; reactivity ratios; ^{13}C nuclear magnetic resonance spectroscopy; monomer unit distribution; chemical heterogeneity; molecular weights; thermal stability)

INTRODUCTION

We recently described the synthesis and the structural and mechanical properties of a series of statistical amorphous copolymers of ethyl acrylate and diethyl-2-(2-methacryloxyethoxy-2-ethyl)-1-(3-sulphopropyl)ammonium betaine¹, which are essentially characterized by a heterogeneous structure. The zwitterionic units tend to self-associate by dipolar interactions in discrete microdomains dispersed in the weakly polar matrix²; these 'clusters', able to dissolve stoichiometric amounts of salts like LiClO_4 , behave as thermally reversible physical crosslinks and thus impart to the material very specific bulk properties analogous to those of a thermoplastic elastomer³. Since the pioneering work of Baer *et al.*⁴ on 'zwitterionic' poly(siloxanes), scarce literature data on other zwitterionic statistical copolymers show analogous trends⁵⁻⁸ and suggest that these materials may already be considered as an interesting and versatile alternative to the well known ionomers⁹⁻¹¹ of identical complexity and technological interest.

However, the comprehensive and quantitative description of the structure of these heterogeneous materials (true physical meaning of the popular 'multiplet' and 'cluster' terms) still remains a major goal, which is far from being reached.

In the present work we focus our attention on amorphous statistical copolymers of n-butyl acrylate (A)



and 1,1-dimethyl-1-(3-methacrylamidopropyl)-1-(3-sulphopropyl)ammonium betaine (B) selected as an optimized system with respect to that involved in our initial studies¹ for at least two reasons:

(i) For an identical dipolar structure, the lower polarity and the higher mobility of the n-butyl acrylate matrix are expected to improve microphase separation and thus to enhance the mechanical properties.

(ii) The industrial availability of the zwitterionic monomer is a very favourable factor for potential technological developments.

In the first part of this series of communications the synthesis and molecular characterization of the copolymers are reported in detail and their resistance to thermal degradation is briefly outlined. In the following f_i refers to the molar fraction of monomer i (molar mass M_i) in the comonomer feed, and F_i and W_i refer to its molar and weight fraction in the copolymer respectively.

* To whom correspondence should be addressed

EXPERIMENTAL

Monomers, reagents and solvents

n-Butyl acrylate was purified by vacuum distillation over CaH_2 and safely stored under argon at -15°C without autopolymerization. Monomer B from Raschig GmbH was used as received without further purification. 4,4'-Azobis-4-cyanovaleric acid (ACVA) was recrystallized according to a literature procedure¹² without separating its two isomers, which do not show a significant difference in their rate of thermal decomposition¹³. Solvents of the best reagent grade were used without further distillation.

Polymerization and kinetic measurements

The monomers, 96 vol% ethanol (previously deoxygenated by refluxing under argon) and initiator were introduced into a Pyrex glass double-walled reactor fitted with a magnetic stirrer and connected with an external Lauda thermostat allowing the temperature to be monitored within $\pm 0.1^\circ\text{C}$. The system was degassed at room temperature by three successive vacuum-argon sweeping cycles and the reaction was then carried out at a constant temperature of 50°C and for a given time under a slight pressure of argon. After addition of a small amount of hydroquinone to stop the polymerization, the solvent and monomer A were stripped off by rotary evaporation.

To eliminate the monomer B, the residual mixture was swollen in water under stirring for 12 h, then exhaustively dialysed for 72 h using cellulosic Spectrapor membranes of molecular cut-off 3500 and finally freeze-dried. The lack of any residual monomer B was checked by thin-layer chromatography (silica gel, Merck 60 F₂₅₄) using 2,2,2-trifluoroethanol (TFE) as deposition solvent and methanol as the eluting one: $R_f(\text{B}) \approx 0.18$, $R_f(\text{copolymers}) \approx 0$. The copolymers are very hygroscopic, especially those of high B content: they must be dried at 80°C under 10^{-2} torr (1.3 Pa) for at least 24 h and stored in a desiccator; they are further dried overnight in the same conditions before any analysis or physical measurements.

For kinetic experiments, the *n*-butyl acrylate consumption was monitored by gas-liquid chromatography using *n*-propanol as internal reference: a Perkin-Elmer 900 gas chromatograph fitted with a dual flame ionization detector and connected with a Hewlett-Packard 3370 B integrator was used. Separation was performed at 100°C on a column of poly(ethylene oxide) (0.230 g) deposited on Chromosorb W ($L = 1.50$ m, $\phi = 1/8$ inch (~ 3 mm)).

Fractionation

The fractionation of copolymer ($W_B = 0.237$) was carried out by precipitation, using ethanol-water as the solvent-non-solvent system in the presence of a constant amount of LiClO_4 (0.8×10^{-2} mol l^{-1}). The coacervation of the successive fractions from the initial polymer solution (1.2 g dl^{-1}) was monitored by a progressive increase of the non-solvent volume fraction (γ) and a simultaneous temperature decrease from 40 to 20°C . Some important fractions were refractionated using the same procedure, starting from a more dilute solution (0.8 g dl^{-1}).

¹³C n.m.r. spectroscopy

¹³C n.m.r. spectra of some copolymers and of their parent homopolymers were recorded on a Bruker AC 200 spectrometer operating at 50.3 MHz (with ¹H decoupling). Measurements were performed on concentrated (15 wt%) TFE solutions (volume fraction of deuterated solvent of about 0.2 for locking) at room temperature. The TFE CH₂ quadruplet (fixed at 126.3 ppm) provides a convenient chemical shift reference. With a flip angle of 90° , a repetition time of 1 s was chosen. Good signal-to-noise ratio was obtained after 20 000 and 80 000 averagings for the homopolymers and the copolymers respectively. The partial deconvolution of the complex carbonyl patterns of the copolymers (analysis of their monomer unit distributions) was performed using the LINESIM program (Bruker) (see 'Results and discussion').

Molecular-weight measurements

Refractive index increments, dn/dc , were measured at room temperature on a Brice Phoenix BP 1000 V differential refractometer using a neon laser beam of $\lambda = 6320 \text{ \AA}$. Depending on the zwitterion content of the copolymers, different solvents were used: 2-methoxyethanol for $W_B < 0.15$ ($dn/dc(A_n) = 0.057$ ml g^{-1}) and TFE for higher B contents. In the latter case, all the copolymer samples obey well the expected additivity relationship $dn/dc = \sum_i W_i (dn/dc)_i$ with $dn/dc = 0.157$ and 0.207 ml g^{-1} for A_n and B_n respectively. Light scattering (LS) experiments were carried out at room temperature on a Sofica 42000 apparatus at the same wavelength.

Gel permeation chromatography (g.p.c.) measurements, restricted to low B content copolymers ($W_B < 0.25$), were performed at 60°C in dimethylformamide (DMF)/LiBr 0.05 mol l^{-1} solutions, on a Waters 150 apparatus fitted with five Hibar columns and calibrated with polystyrene standards.

Thermogravimetry

Measurements were carried out on 30–50 mg of finely ground samples under a constant nitrogen flow (200 ml min^{-1}) and a heating rate of 5 K min^{-1} using a Mettler TA/3000 thermobalance.

RESULTS AND DISCUSSION

Radical copolymerization kinetics, reactivity ratios, monomer unit distribution and compositional heterogeneity

Radical copolymerization of monomers A and B was systematically performed in 96 vol% ethanol solution at 50°C under the following conditions:

$$1 \leq [A + B] \leq 2.9 \text{ mol l}^{-1}$$

$$[\text{ACVA}] = 1 \times 10^{-3} \text{ mol l}^{-1}$$

The reaction medium remains homogeneous throughout the copolymerization only for low monomer B contents, $f_B < 0.1$; the copolymer precipitates in the other cases. Conversion (τ) was systematically limited to less than 20% to avoid too high a compositional heterogeneity of the resulting copolymers (see later). In some cases, an induction period (20–30 min) occurred, but its variations cannot be correlated with any copolymerization variable such as the unpurified monomer B content for instance, and this adventitious feature has no

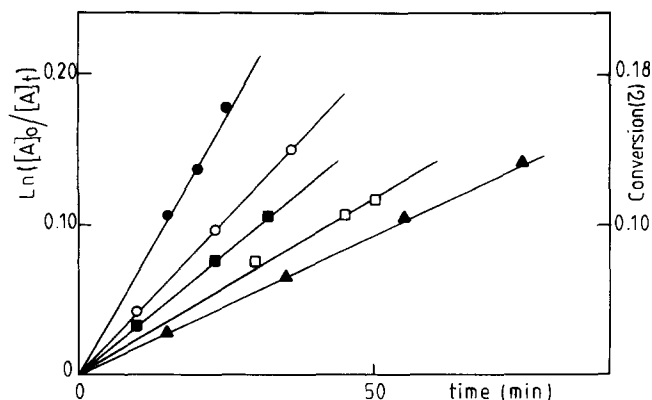


Figure 1 First-order consumption of *n*-butyl acrylate in copolymerization for various initial monomer feed compositions, $f_B = 0$ (●), 0.017 (○), 0.040 (■), 0.051 (□), and 0.1 (▲)

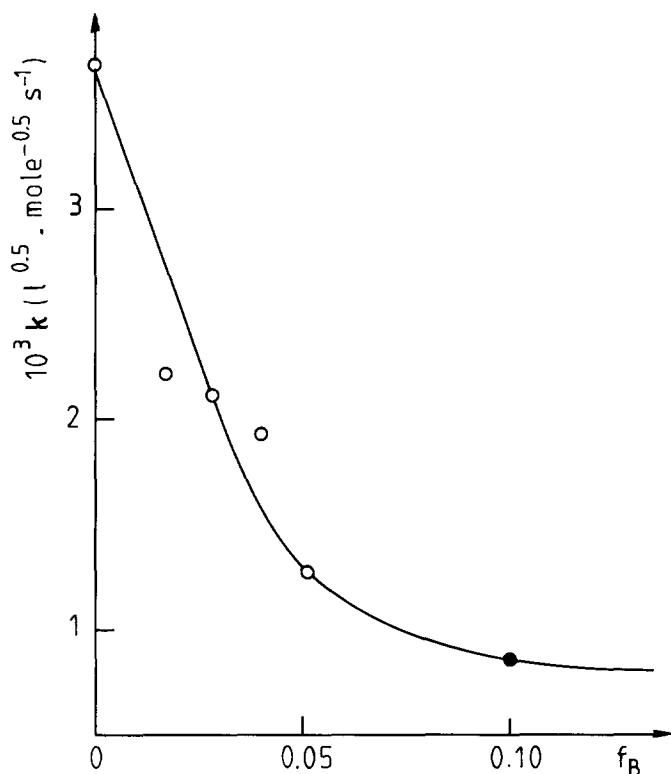


Figure 2 Variation of the apparent first-order rate constant k of *n*-butyl acrylate consumption with initial monomer feed composition: homogeneous phase (○); heterogeneous phase (●)

influence on any of the following experimental results. The initial consumption of *n*-butyl acrylate studied only for B-poor monomer feeds ($f_B < 0.1$, $[A + B] = 1 \text{ mol l}^{-1}$) obeys first-order kinetics as shown in Figure 1. This allows the derivation of an apparent pseudo-first-order rate constant k as defined by:

$$\ln([A]_0/[A]_t) = k[ACVA]_0^{0.5}t$$

k decreases by a factor 3 when going from $f_B = 0$ to $f_B = 0.05$ and then tends to level off (see Figure 2): this behaviour is similar to that previously observed in the ethyl acrylate–zwitterionic methacrylate monomer pair polymerized under nearly identical experimental conditions¹.

Copolymer composition was derived from elemental analysis, and self-consistent and reliable values were

obtained from both nitrogen and sulphur microanalysis over the whole composition range as shown below:

$\bar{F}_B(S)$	0.121	0.271	0.482
$\bar{F}_B(N)$	0.119	0.276	0.496

The reactivity ratios were thus derived from a series of experiments covering a wide range of monomer feed composition ($0 < f_B \leq 0.65$) using the Kelen–Tüdös method¹⁴, which takes into account the degree of conversion, τ . Calculations show that there is no reason to consider separately the homogeneous and heterogeneous reactions: all the data are reasonably linearized (correlation coefficients $R(12) = 0.964$), leading to the following reactivity ratios: $r_A = 0.42$, $r_B = 6.00$ (see Figure 3). For very low B content of the comonomer feed, $f_B < 0.1$, the copolymer composition may be readily approximated by the simple linear relation: $\bar{F}_B = 2.31f_B^0 + 0.005$; $R(10) = 0.989$.

Because of the very high polarity contrast between the two monomers ($\mu_A \approx 1.72 \text{ D}^{15}$ and $\mu_B \approx 25 \text{ D}$ for triethylammonium sulphopropylbetaine¹⁶) the propagation step may involve preferential solvation of the growing macroradicals by a given reactive species, in such a way that the analysis of compositional data may lead only to ‘apparent’ reactivity ratios, which do not reflect the true chain microstructure¹⁷. Such complications may worsen in the heterogeneous systems ($f_B > 0.1$). The calculated distribution of A and B units along the chain was thus checked at an experimental level using ¹³C n.m.r. spectroscopy. The carbonyl patterns are the most suited to our purpose and some representative spectra obtained in TFE solution (see ‘Experimental’) are given in Figure 4a. Configurational effects, barely apparent for A_n in good agreement with literature data¹⁸, strongly broaden the CO peak of B_n . The overlapping contributions of compositional and configurational effects and the rather

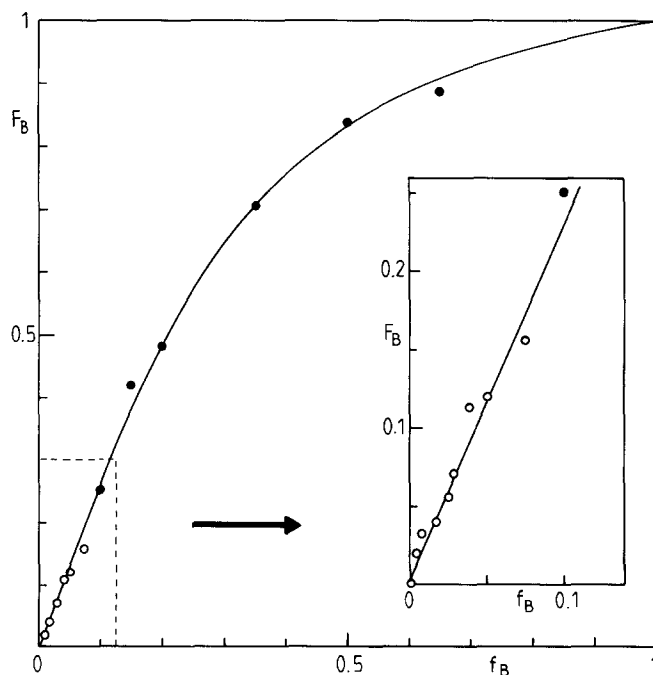


Figure 3 Composition diagram of the A–B copolymerization system: homogeneous phase (○); heterogeneous phase (●). The instantaneous composition curve is calculated for $r_A = 0.42$ and $r_B = 6.0$ (—)

poor resolution of the spectra do not allow complete identification and quantitative estimation of the various A- and B-centred triads. However, partial deconvolution (see Figure 4b) of the CO pattern was performed using the progressive evolution of the spectra and the composition data derived from elemental analysis as guidelines ($\bar{F}_B = \overset{*}{B}\overset{*}{B}\overset{*}{B} + \overset{*}{B}\overset{*}{B}\overset{*}{A} + \overset{*}{A}\overset{*}{B}\overset{*}{A}$). Comparison of the calculated¹⁹ and experimental distribution is given in Table 1: the good agreement observed over the whole composition range for some A and B specific triads shows that the values of the reactivity ratios are reliable and physically meaningful, and that deviations of the copolymerization process from the terminal model unit, if any, are negligible under our experimental conditions (potential preferential solvation effects may reasonably be expected to increase with conversion).

The drastically higher rate of monomer B consumption implies an increased compositional heterogeneity of the samples with increasing conversion. The instantaneous F_B and the cumulative \bar{F}_B composition of the copolymers calculated according to the Meyer and Lowry equation²⁰ are plotted as a function of conversion τ for some representative monomer feeds in Figure 5. Compositional drift is never negligible, more especially for the B-poor monomer feeds of interest in the synthesis of the 'zwitterionomers' selected for physical studies. Compositional polydispersity was thus tentatively analysed at an experimental level choosing a copolymer sample obtained in homogeneous solution ($f_B = 0.051$, $\tau = 0.11$, $\bar{F}_B = 0.120$ or $W_B = 0.227$, $\bar{M}_w = 1.12 \times 10^5$). We were unable to find solvent–non-solvent systems necessary to carry out 'cross-fractionation', which has been shown to be most efficient and reliable to estimate chemical heterogeneity in copolymers²¹, and fractionation was thus performed in 'one direction' as described in the 'Experimental' part. The fairly good agreement between the average composition of the original copolymer and that of the cumulated recovered fractions ($\sum_i w_i W_B^i = 0.223$) shows that unavoidable material losses during fractionation (yield of 88%) are not selective. The cumulative distribution curve given in Figure 6 is symmetrical (symmetry factor²¹ $V = 1.02$) and fairly narrow: mean-square standard deviation $\sigma^2 = 2.4 \times 10^{-4}$. The apparent σ^2 value calculated for a hypothetical homogeneous

copolymer of the same composition and fractionated in the same way may be estimated as about 2.2×10^{-5} assuming that the accuracy of the composition of the various fractions is about $\pm 2\%$. Thus the tenfold higher experimental σ^2 value reflects a true but weak and probably underestimated heterogeneity, of the same order as that observed for an azeotropic styrene–methyl methacrylate copolymer for instance²². This result is in good agreement with previous calculations taking into account that copolymerization conversion was restricted to a low value of $\tau = 0.11$ (see Figure 5).

Molecular weights and dilute solution properties

The copolymers retain the solubility properties of poly(*n*-butyl acrylate) in tetrahydrofuran (THF), acetone and 2-methoxyethanol only for $F_B < 0.07$ and become water-soluble at 50°C for $F_B > 0.85$ while B_n is water-soluble at room temperature. However, all the samples can be readily dissolved in fluorinated alcohols such as trifluoroethanol (TFE) for instance. Because of the good chemical homogeneity of the samples, the apparent weight-average molecular weights derived from light scattering experiments may be considered identical to the absolute ones²³, more especially when measurements are carried out in solvents like TFE where A_n and B_n have very high refractive index increments²¹ (see 'Experimental' part). G.p.c. experiments were restricted to copolymers of low B content ($F_B < 0.13$) soluble in DMF/0.05 N LiBr at 60°C. They essentially lead to unimodal distributions characterized by polydispersity indices \bar{M}_w/\bar{M}_n in the range 1.7–2.2 and to apparent \bar{M}_w values (polystyrene calibration) slightly lower than the previous ones: \bar{M}_w (g.p.c.) $\simeq 0.90\bar{M}_w$ (LS). Fractionation by precipitation, as described above, allows one to isolate chemically homogeneous samples of symmetric and relatively narrow distribution ($\bar{M}_w/\bar{M}_n \simeq 1.3$).

Figure 7 shows the influence of the initial monomer feed composition on weight-average degrees of polymerization DP_w^* (LS) normalized to standard conditions ($[A + B] = 1 \text{ mol l}^{-1}$; $[ACVA] = 1 \times 10^{-3} \text{ mol l}^{-1}$):

$$DP_w^* = \frac{M_w}{M} \frac{1}{[A + B]} \left(\frac{[ACVA]}{10^{-3}} \right)^{0.5}$$

with $M = M_A \bar{F}_A + M_B \bar{F}_B$.

Table 1 Compositional triad distributions for AB polymers: comparison between experimental and calculated values

Copolymer composition, $\bar{F}_B \times 100$		$\overset{\bullet}{B}$ -centred triads			$\overset{\bullet}{A}$ -centred triads		
		$\overset{\bullet}{B}\overset{\bullet}{B}\overset{\bullet}{B}$	$\overset{\bullet}{B}\overset{\bullet}{B}\overset{\bullet}{A}$	$\overset{\bullet}{A}\overset{\bullet}{B}\overset{\bullet}{A}$	$\overset{\bullet}{B}\overset{\bullet}{A}\overset{\bullet}{B}$	$\overset{\bullet}{B}\overset{\bullet}{A}\overset{\bullet}{A}$	$\overset{\bullet}{A}\overset{\bullet}{A}\overset{\bullet}{A}$
		181.8	180.6	180.0	179.4	178.8	178.8
		179.2	179.6	178.9	178.2	177.8	177.0
		ppm	ppm	ppm	ppm	ppm	ppm
12.0	Calc.	0.6	4.2	7.2	0.9	16.7	70.4
	Exp.	–	4	8	16		72
27.3	Calc.	4.6	13.1	9.6	2.9	25.4	44.4
	Exp.	5	21		27		47
48.9	Calc.	17.6	23.5	7.8	7.2	24.0	19.9
	Exp.		52			48	
74.3	Calc.	46.8	24.5	3.0	9.3	12.3	4.1
	Exp.		70			30	
88.6	Calc.	71.7	15.9	0.9	6.9	4.0	0.6
	Exp.	66	23		7	4	–

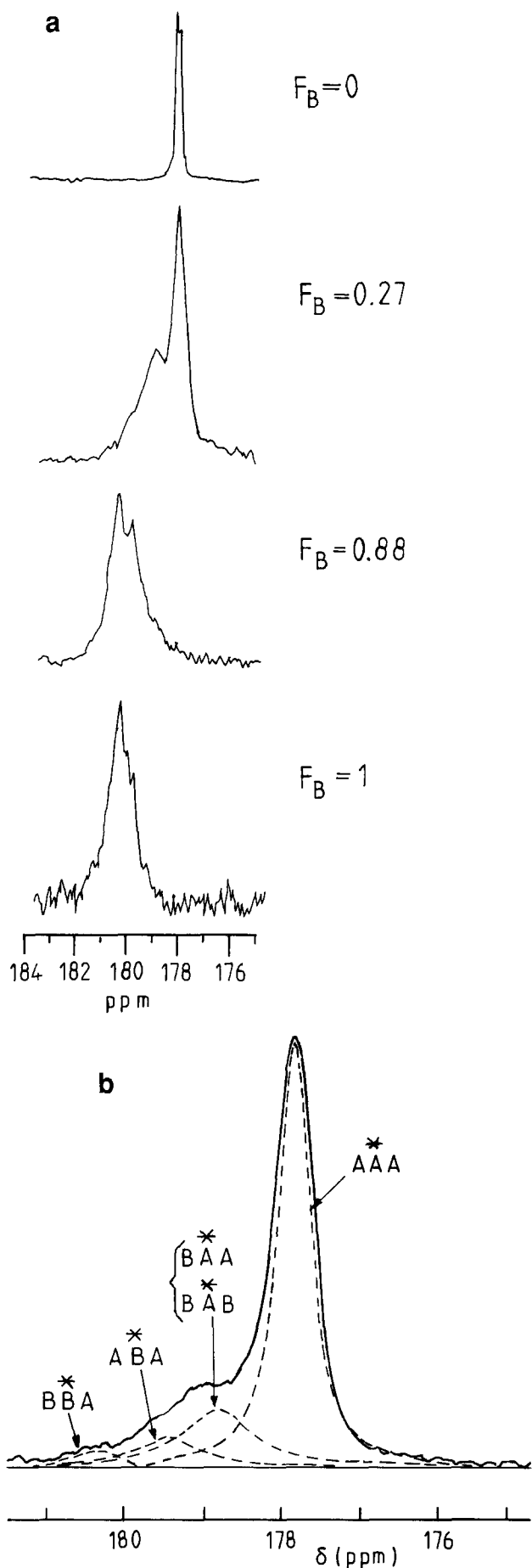


Figure 4 (a) ^{13}C n.m.r. patterns of the carbonyl group for the homopolymers A_n and B_n and for two representative copolymers. (b) Deconvolution of the carbonyl group resonance pattern for the copolymer $F_B = 0.12$

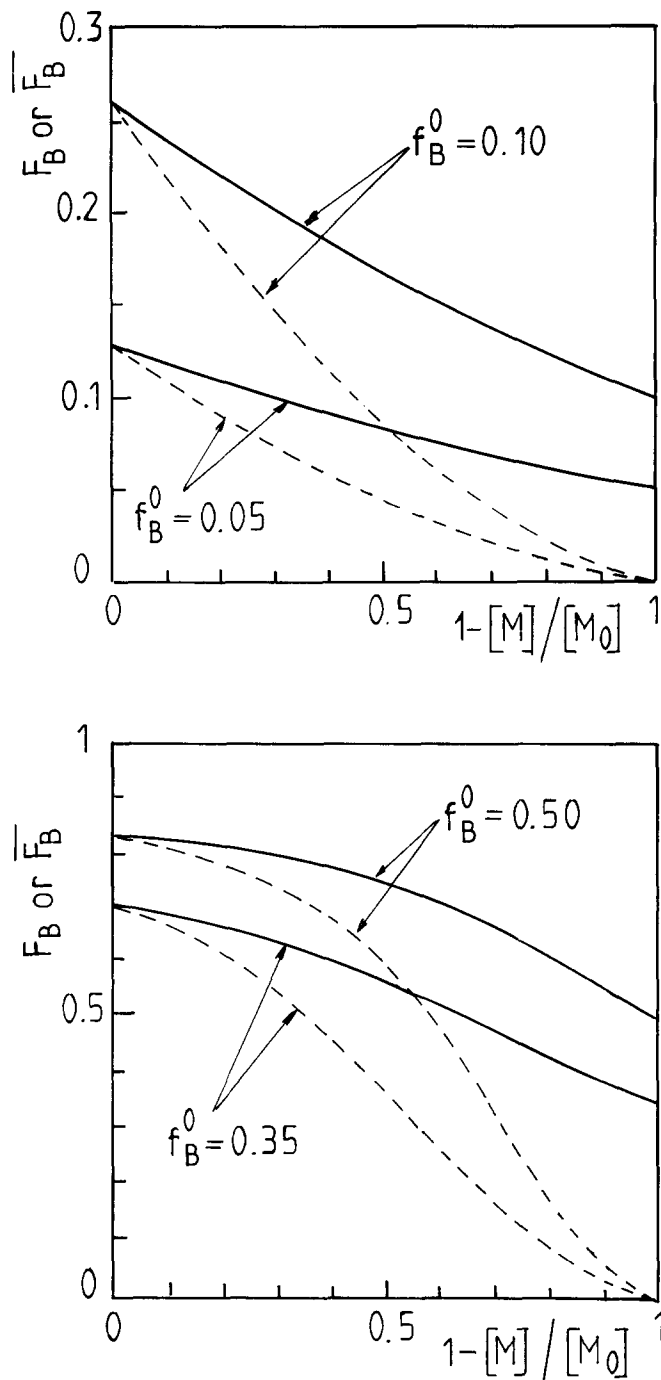


Figure 5 Variation of the instantaneous F_B (---) and cumulative \bar{F}_B (—) copolymer compositions with total mole conversion for various initial monomer feeds

The transition from a homogeneous to a heterogeneous system for $f_B \approx 0.1$ results in a rather sharp increase in the chain length of the copolymer by a factor of about 2.3, while its fluctuations with monomer feed composition within either of these two clearly separated domains are not significant.

The influence of composition on the dilute solution properties of the copolymers in TFE solution were briefly analysed for six samples showing negligible fluctuations in weight-average degree of polymerization: $DP_w^- = 2100 \pm 200$. Fluorinated alcohols are the most powerful hydrogen bond donors²⁴ and are already well known to be the thermodynamically best solvents for poly(methyl methacrylate)²⁵ and poly(ammonium sulphopropylbetaines)²⁶ through strong hydrogen bonding to their carbonyl and sulphonate sites respectively. The very high

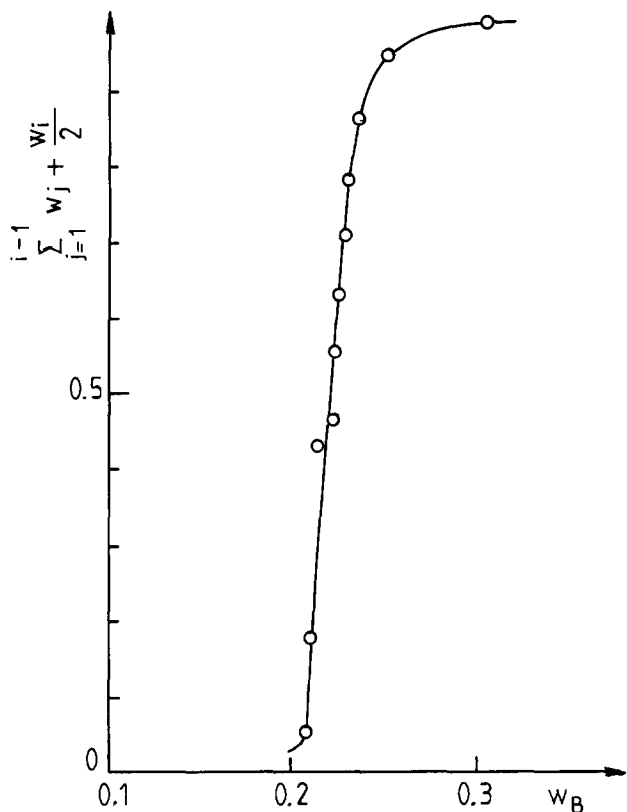


Figure 6 Cumulative compositional distribution curve of copolymer $F_B = 0.12$

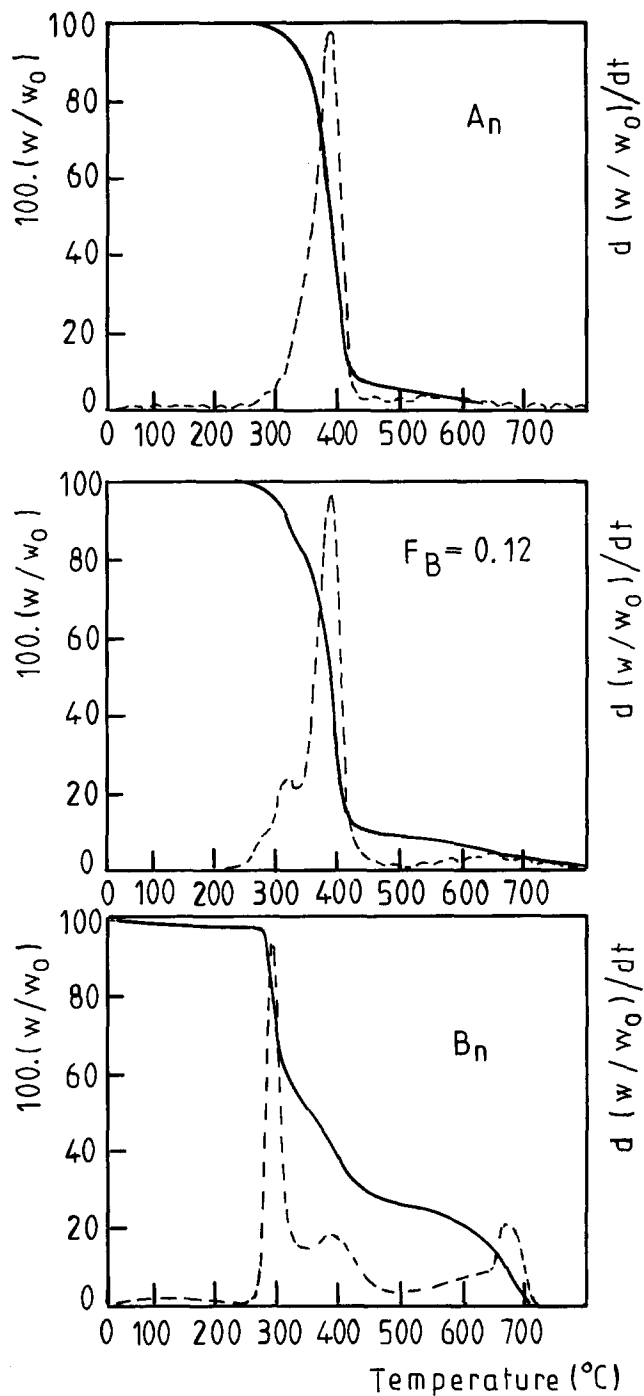


Figure 9 Thermogravimetric analysis of the homopolymers A_n and B_n and of a representative copolymer ($F_B = 0.12$) under nitrogen. Residual weight $(w/w_0) \times 100$ (—) and derivative trace (---) versus temperature T

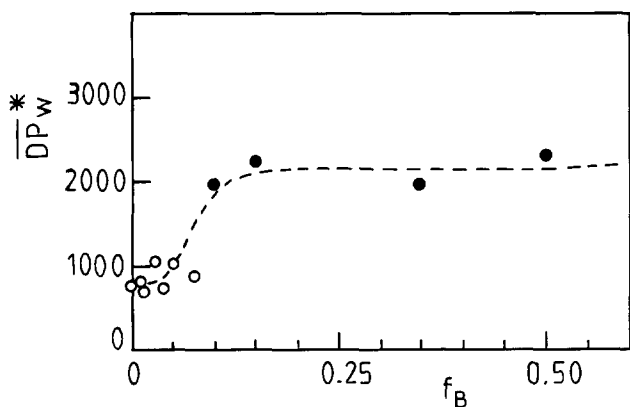


Figure 7 Variation of the normalized weight-average degree of polymerization \overline{DP}_w^* of the copolymer with initial monomer feed composition: homogeneous phase (○); heterogeneous phase (●)

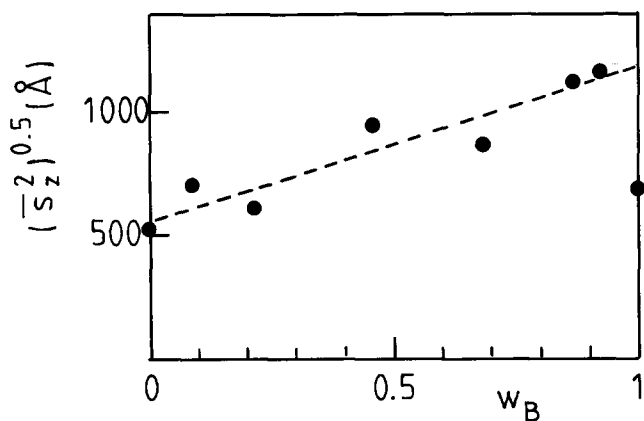


Figure 8 Variation of the radius of gyration $(S_z^2)^{0.5}$ of the copolymer with composition, as measured in TFE solution (room temperature) for chains of constant \overline{DP}_w^* (2100 ± 200)

experimental values of both the second virial coefficients (2×10^{-3} to 2×10^{-2} mol ml g⁻²) and of the radius of gyration ($(S_z^2)^{0.5} \approx 600\text{--}1200$ Å) are thus not surprising. Moreover, the copolymers' coils appear more expanded than those of their parent homopolymers of the same \overline{DP}_w^* as a result of strong intramolecular repulsion between incompatible A and B segments within the chain: see Figure 8.

Thermal stability

The comparison of the thermal stability of a representative copolymer ($F_B = 0.12$) and of the parent homopolymers was performed by thermogravimetric (t.g.) analysis carried out under a nitrogen atmosphere

Table 2 Thermal degradation of a copolymer and of its parent homopolymers under nitrogen atmosphere

Polymer	T_i^a (°C)	Temperature range (°C)	Weight loss (%)	Activation energy (kJ mol ⁻¹)
A_n	325	340–385	9–46	126
		385–410	46–85	166
AB ($F_B = 0.12$)	300	267–323	1–11	103
		333–363	14–26	54
		378–410	37–82	140
B_n	285	280–295	3–20	365
		310–425	37–68	15

(see 'Experimental' part). Three representative t.g. curves, giving the variations of the ratio of the sample weight w at temperature T to its initial value w_0 versus temperature and the first derivatives $d(w/w_0)/dt$ vs. T , are shown in Figure 9. The derivative traces clearly show that degradation involves a multistep process, especially in the zwitterionic chains, which appear less stable than pure poly(*n*-butyl acrylate): see Table 2 for the initial degradation temperature, T_i , arbitrarily taken for a weight loss of 5%. Assuming first-order kinetics for the degradation process, an apparent overall activation energy E_a may be estimated within a given temperature range according to the following equation²⁷:

$$\ln\left(-\frac{\ln(1-\alpha)}{T^2}\right) = \ln\left[\left(\frac{AR}{\theta E_a}\right)\left(1 - \frac{2RT}{E_a}\right)\right] - \frac{E_a}{RT}$$

where α is the polymer fraction volatilized at temperature T ($\alpha = (w_0 - w)/w_0$), θ is the heating rate and A is the Arrhenius frequency factor. Linearization of the experimental data leads to the results given in Table 2. The calculated apparent activation energies have to be considered quite cautiously, since they depend strongly on the assumed reaction order, and a detailed analysis of the degradation process is beyond the scope of the present work. However, comparison of the thermal stability of the poly(zwitterion) B_n with that of its homologue poly[dimethyl-2-(2-methacryloyloxyethyl)-1-(3-sulphopropyl)ammonium betaine] bearing the same dipolar structure²⁸ remains of interest. The methacrylate chain appears slightly more stable ($T_i \approx 300^\circ\text{C}$), and for the same weight loss of 70% reached at a temperature of 400°C , degradation occurs according to a single first-order process with an activation energy of 103 kJ mol^{-1} : this is in sharp contrast with the experimental two-step degradation obtained with the methacrylamide polymer.

CONCLUSIONS

In spite of potential complications arising from the high contrast of polarity between the two monomers and from the insolubility of the resulting copolymer in the reaction medium, the radical copolymerization of *n*-butyl acrylate (A) and 1,1-dimethyl-1-(3-methacrylamidopropyl)-1-(3-sulphopropyl)ammonium betaine (B) in ethanol solution at 50°C apparently obeys the simple terminal unit model over the whole composition range: $r_A = 0.42$, $r_B = 6.00$. When restricted to low enough conversion ($< 20\%$), it readily leads to high-molecular-weight copolymers of good chemical homogeneity and reasonable molecular-weight distribution ($\bar{M}_w/\bar{M}_n \approx 2$). The study of micro-phase separation in these 'pseudo-ionomers' and of their dynamic mechanical properties will be described in further communications.

ACKNOWLEDGEMENTS

The authors gratefully acknowledge Rhône-Poulenc for a grant to one of us (Marc Ehrmann), for g.p.c. measurements (Centre de Recherches d'Aubervilliers) and for fruitful discussions with Drs D. Charmot, J. C. Daniel and R. Reeb. They are indebted to Dr M. Galin for kinetic measurements, to M. Y. Guilbert for thermogravimetric analysis and n.m.r. spectroscopy and to Mrs H. Bellissent for her efficient technical assistance.

REFERENCES

- Zheng, Y. L., Galin, M. and Galin, J. C. *Polymer* 1988, **29**, 724
- Mathis, A., Zheng, Y. L. and Galin, J. C. *Makromol. Chem., Rapid Commun.* 1986, **7**, 333
- Bazuin, C. G., Zheng, Y. L., Muller, R. and Galin, J. C. *Polymer* 1989, **30**, 654
- Graiver, D., Litt, M. and Baer, E. J. *Polym. Sci., Polym. Chem. Edn.* 1979, **17**, 3573, 3607, 3625
- Neculescu, C., Clough, S. B., Elayaperumal, P., Salamone, J. C. and Watterson, A. C. *J. Polym. Sci., Polym. Lett. Edn.* 1985, **25**, 201
- Clough, S. B., Cortelek, D., Nagabhushanam, T., Salamone, J. C. and Watterson, A. C. *Polym. Eng. Sci.* 1984, **24**, 385
- Salamone, J. C., Elayaperumal, P., Clough, S. C., Watterson, A. S. and Bibbo, M. A. *Am. Chem. Soc. Polym. Prepr.* 1986, **27**, 323
- Hamaide, T., Le Percec, P., Verney, V. and Guyot, A. in 'Structure and Properties of Ionomers' (Eds. M. Pineri and A. Eisenberg), NATO ASI Ser. C, Vol. 198, Reidel, Dordrecht, 1987, p. 529
- Eisenberg, A. and King, M. 'Ion-Containing Polymers', Academic Press, New York, 1977
- MacKnight, W. T. and Earnest, T. R. Jr. *J. Polym. Sci., Macromol. Rev.* 1981, **16**, 41
- Bazuin, C. G. and Eisenberg, A. *Ind. Eng. Chem., Prod. Res. Dev.* 1981, **20**, 271
- Bamford, C. H., Jenkins, A. D. and Wayne, R. P. *Trans. Faraday Soc.* 1960, **56**, 932
- Overberger, C. G. and Labianca, A. D. *J. Org. Chem.* 1970, **35**, 1762
- Tüdös, F., Kelen, T., Földes-Bereznich, T. and Turesányi, B. *J. Macromol. Chem. (A)*, 1980, **10**, 1513
- McClellan, A. L. 'Tables of Experimental Dipole Moments', Raha Enterprises, California, 1989, Vol. 3, p. 375
- Chapoton, A. and Galin, M., unpublished results
- Harwood, H. J. *Makromol. Chem., Macromol. Symp.* 1987, **10/11**, 331
- Llauro-Darricades, M. F., Pichot, C., Guillot, J., Rios, L. G., Cruz, M. A. E. and Guzman, C. C. *Polymer* 1986, **27**, 889
- Ito, K. and Yamashita, Y. *J. Polym. Sci. (A)* 1965, **3**, 2165
- Meyer, V. E. and Lowry, G. G. *J. Polym. Sci. (A)* 1965, **3**, 2843
- Bourguignon, J. J., Bellissent, H. and Galin, J. C. *Polymer* 1977, **18**, 937
- Teramachi, S. and Kato, Y. *Macromolecules* 1971, **4**, 54
- Benoit, H. and Froelich, D. 'Light Scattering from Polymer Solutions' (Ed. M. G. Huglin), Academic Press, London, 1972, p. 467
- Taft, R. W., Abboud, J.-L. M., Kamlet, M. J. and Abraham, M. H. *J. Solution Chem.* 1985, **14**, 153
- Hamori, E., Prusinowski, L. R., Sparks, P. G. and Hughes, R. E. *J. Phys. Chem.* 1965, **69**, 1101
- Monroy-Soto, V. M. and Galin, J. C. *Polymer* 1984, **25**, 254
- Coats, A. W. and Redfern, J. P. *Nature* 1964, **201**, 68
- Der-Jang Liaw and Wen-Fu Lee *J. Appl. Polym. Sci.* 1985, **30**, 4697